periods N. Thus, the net transfer decreases for both a *decrease* in N and an increase in amplitude b.

Our results show net diffusive transfer is somewhat decreased (proportional to ϵ^2) by corrugations if the *perimeter length is fixed.* However, from Figure 3 we see that corrugations may also cause a large reduction in the maximum dimensions. Thus, for *given maximum dimensions*, although the net transfer is decreased by corrugations, this decrease may be more than offset by a concurrent increase in perimeter length. This is exemplified by the microvilli in the digestive tract and hollow core cooling fins on heat engines. We must keep in mind that corrugations may not automatically increase net transfer for given maximum dimensions. There may be cases where large ϵ, λ, a or b cause such a decrease in net transfer that cannot be compensated by the concurrent increase in perimeter length. One must make a careful calculation using the results of this paper.

Since our perturbation Eq. 23–25 are linear in k, our present method may be extended to any periodic curvature

$$k = a + \sum b_n \cos\lambda ns. \tag{41}$$

Lastly, the present analysis can be applied to various kinds of diffusive transfer other than the flow of heat, mass or concentration. One example is the electric potential distribution inside corrugated capacitor plates. Another instance is the $\mathbf{k}$ direction parallel motion of corrugated plates separated by a viscous fluid. Both problems are governed by Eqs. 5 and 6.

NOTATION

a	= mean curvature
b	= amplitude of corrugation
d	= ½ thickness
D	= diffusion coefficient
f,g,h	= functions of s,η
G	= function of λ,a,b
k	= scaled curvature
$\mathbf{k}$	= unit vector in z direction
K	= curvature
ℓ,m	= functions of η
n	= integer
N	= N-fold symmetry
$\mathbf{N}$	= unit normal
Q	= net transfer
$\mathbf{R}$	= position vector of centerline
s	= arc length
$\mathbf{T}$	= unit tanget
T	= concentration of diffuser
$\mathbf{x}$	= position of vector
x,y,z	= Cartesian coordinates

Greek Letters

β	= b'/a'
ϵ	= small number
η	= normal coordinate
θ	= local angle of inclination of centerline
λ	= frequency of corrugation

Superscripts

= dimensional quantity
= quantity renormalized with respect to b'

LITERATURE CITED

Crank, J., *The Mathematics of Diffusion*, Clarendon Press, Oxford (1956).

Goldstein, S., *Modern Developments in Fluid Dynamics*, **1**, Clarendon Press, Oxford, 119 (1938).

Morse, P. M., and H. Feshbach, *Methods of Theoretical Physics*, **1**, McGraw-Hill, New York (1953).

Wang, C.-Y., "Flow in Narrow Curved Channels," *J. Appl. Mech.* **47**, 7–10 (1980).

Manuscript received August 4, 1981; revision received October 19, and accepted November 5, 1981.

Model of Solid Gas Reaction Phenomena in The Fluidized Bed Freeboard

L. H. CHEN and C. Y. WEN

Department of Chemical Engineering
West Virginia University
Morgantown, WV 26506

A comprehensive model incorporating elutriation, entrainment and reaction is presented to describe the chemical reaction and hydrodynamics occurring in the freeboard of a fluidized bed. A comparison of experimental data on the amount of particles elutriated and the concentration profiles of SO_2 and NO_x obtained from the freeboard of fluidized bed coal combustion (FBC) by the Babcock & Wilcox Company with the calculation based on the proposed model to include the effect of interaction among the entrained particles is desirable. More experimental data with chemical reactions in the freeboard are needed to validate the model for applications to fluidized bed catalytic reactors.

SCOPE

When bubbles burst at the fluidized bed surface, particles are entrained in the freeboard region. The entrained particles with a terminal velocity greater than the actual gas velocity will reach a certain height within the freeboard before they fall back into the bed. However, those particles with a terminal velocity smaller than the actual gas velocity will be elutriated and carried out of the bed. Because of good solid-gas contact in the

C. Y. Wen is deceased.

0001-1541-82-5468-1019-$2.00.

freeboard region, the reaction in this region may be significant in many instances and may not be neglected.

Several models have been proposed for the fluidized bed freeboard reaction (Miyauchi and Furusaki, 1974; Ford et al., 1977; Yates and Rowe, 1977; deLasa and Grace, 1979; Beer et al., 1980; Rajan and Wen, 1980). However, those models have been either based on too simplified solid entrainment phenomena or require additional experimental measurements to determine the parameters.

It is the objective of this study to examine the mechanism of solid entrainment in the fluidized bed freeboard region and to develop a freeboard model describing solid-gas reactions incorporating entrainment and elutriation correlations developed earlier (Wen and Chen, 1981).

CONCLUSIONS AND SIGNIFICANCE

The solid hold-up in the fluidized bed freeboard region has been calculated from the solid entrainment rate as well as the solid velocity in the freeboard. For the case in which the solid hold-up is important in determining the reaction rate, such as in the catalytic gas phase reaction and in the non-catalytic solid-gas reaction, the freeboard region provides additional opportunities for intimate solid-gas contacting.

It has been shown that a considerable amount of reactions of SO_2 absorption and NO_x reduction take place in the freeboard of the Babcock and Wilcox (B & W) 6 ft × 6 ft (1.8 m × 1.8 m) fluidized bed combustor. Any method that will increase the solid hold-up in the freeboard without excessive carryover, such as recycling the fine particles back to the bed, should improve considerably the SO_2 absorption and NO_x reduction in the operation of fluidized bed coal combustors.

INTRODUCTION

As the entrained particles are thrown up by the bubbles and gas stream from the fluidized bed surface, they will either rise or fall in the freeboard, depending on the size and density of the particles and the gas velocity. Those particles with terminal velocity greater than the gas velocity (coarse or large particles) will reach a certain height within the freeboard before falling back to the bed. However, those particles with terminal velocity smaller than the gas velocity (fine or small particles) will, eventually, be carried out of the bed or elutriated. During the solid- gas disengagement process, additional particles may also fall down if they hit the wall. Wen and Hashinger (1960), based on their elutriation experiments, postulated that a substantial amount of the fine particles fall down along the wall. Horio et al. (1980) observed a descending zone near the wall for fine particles. They reported that the thickness of the descending zone near the wall is greatest adjacent to the bed surface but decreases as it moves away from the bed surface.

The sailing of fine particles to the wall was attributed to the gas flow pattern in the freeboard region (Wen and Hashinger, 1960; Horio et al., 1980). At the lower part of the freeboard, gas turbulence has a considerable effect on the entrainment of fine particles. The gas turbulence, which results from bursting of bubbles at the bed surface, causes the lateral movement of fine particles from the ascending to the descending zone near the wall (Horio et al., 1980). However, in the upper portion of the freeboard, the effect of the gas turbulence diminishes. As a more well developed gas velocity profile, either laminar or turbulent flow, is generated far above the bed surface, the fine particles situated near the wall where the gas velocity is very low would fall down along the wall (Wen and Hashinger, 1960). The gas flow pattern at 3.66 m above the fluidized FCC catalyst bed surface was measured by Fournol et al. (1973). The bed was fluidized at a velocity of 0.15~0.16 m/s. Under this condition, the Reynolds number for the gas flowing through the column is well above the transition point between laminar and turbulent flow (5,830 ~ 6,400 > 2,100). The gas velocity profile in the radial direction was measured to be relatively flat (D_c = 0.61 m) and exhibited the shape characteristic of turbulent flow, as was expected.

The exponential decrease of the solid entrainment rate along the freeboard for fine particles can be mainly attributed to the wall (Horio et al., 1980). For large particles, however, the initial solid velocity distribution plays a more important role in the decrease of solid entrainment rate (George and Grace, 1978).

The importance of freeboard region in a fluidized bed reactor has been shown by several investigators (Miyauchi and Furusaki, 1974; Ford et al., 1977; Yates and Rowe, 1977; de Lasa and Grace, 1979). For a fast reaction, the freeboard region could contribute 50% or more in the overall conversion of the gas phase catalytic reaction (Yates and Rowe, 1977). However, the freeboard reaction models proposed have been either based on simplified solid entrainment phenomena or require experimental measurement of the parameters. For example, in the model proposed by Miyauchi and Furusaki (1974), it is required to determine experimentally the solid concentration profile along the freeboard. Yates and Rowe (1977), on the other hand, assumed a constant solid concentration profile in the freeboard. Recently, a freeboard model for the fluidized bed catalytic cracking regenerator was proposed by de Lasa and Grace (1979), based on a mechanistic solid entrainment model. The freeboard solid concentration profile in their model calculated appears to increase rather than decrease with the freeboard height before its leveling off high above the bed surface. This kind of solid concentration profile appears to be unrealistic (Matsen, 1979). Rajan and Wen (1980), in their fluidized bed coal combustor model, assumed an exponential decrease in the solid entrainment rate from the bed surface to the TDH. But, the solid velocity for a close-cut particle size was approximated by a constant value. This is inconsistent with the assumption of the exponential decay in the solid entrainment rate.

The gas flow pattern for the freeboard is another factor that may affect the concentration profiles of the reactants in the freeboard. Most of the investigators (Miyauchi and Furusaki, 1974; Yates and Rowe, 1977; de Lasa and Grace, 1979; Beer et al., 1980) used either a plug flow or complete-mixing flow model. Rajan and Wen (1980), on the other hand, assumed the equal-sized compartment-in-series model or the axial dispersion model for the gas hydrodynamics in the freeboard. In the present study, the axial dispersion model is used based on the experimental results of Horio et al. (1980) who observed that there is an evidence of some degree of backmixing of the gas in the freeboard region.

MODEL DEVELOPMENT

Entrainment Mechanism

For the solid-gas reaction, the solid hold-up or concentration in the freeboard will affect the reaction rate. To calculate the solid hold-up, it is necessary to know both entrainment rates and velocities of solid particles. The solid entrainment rate calculation has been shown as follows: (Wen and Chen, 1981)

$$F_i = F_{i\infty} + (F_{io} - F_{i\infty}) \exp(-ah) \quad (1)$$

Solid Velocity. When bubbles burst at the bed surface the particles are thrown upwards with different initial velocities. The axial velocity profiles in the freeboard for both coarse and fine particles can be obtained from the equation derived based on the forces balance. A balance of drag force, gravitational force, buoyancy force and inertia force for an upward-moving particle is shown as follows: (Zenz and Weil, 1958; Do et al., 1972)

$$\frac{dU_{si}}{dh} = -\frac{3}{4}\frac{C_D \rho_g U_{sr}|U_{sr}|}{\rho_s d_{pi} U_{si}} - \frac{(\rho_s - \rho_g)g}{\rho_s U_{si}} \quad (2)$$

Here, U_{sr} $(= U_{si} - U_g)$ is the relative velocity of the particle to the gas stream. C_D, the drag coefficient for multiparticle system, is represented by the following equation: (Wen, 1971; Wen and O'Brien, 1976)

$$C_D = C_{DS} \cdot \epsilon^{-4.7} \quad (3)$$

C_{DS}, the drag coefficient for single particle, can be calculated from the following equation suggested by Do et al. (1972).

$$C_{DS} = \frac{24}{N_{Re}}(1 + 0.15 N_{Re}^{0.687}) + \frac{0.42}{1 + 4.25 \times 10^4 N_{Re}^{1.16}} \quad (4)$$

U_g, the average gas velocity, is estimated from the superficial gas velocity as follows:

$$U_g = U_o/\epsilon \quad (5)$$

where, ϵ, the voidage in the freeboard, is related to the solids hold-up. At each height, h, the value of ϵ is assumed first to calculate gas, solid velocities and particles hold-up. The assumed value of ϵ will then be checked with the calculated value of ϵ from the particle hold-up. Iteration will be performed until these two values agree. The detail method for calculation of solids hold-up will be discussed in the later section.

Large particles, when projected from the bed surface, will reach a maximum height where the solid velocity changes from an upward direction to a downward direction. The maximum projected height of the large particle can be calculated from Eq. 2. At this maximum height, the solid velocity is zero.

After reaching the maximum height, the particle falls downwards at an accelerated velocity. Since the total downward-traveling distance is so much greater than the short distance needed for acceleration, the falling velocity of the particle can be assumed to be $(U_{ts} - U_o)$. For the small particles that fall down along the wall, the freefalling terminal velocity, U_{tsi}, of the particle is used for the calculation (Wen and Hashinger, 1960).

The initial solid velocity or the solid velocity at the bed surface for a given particle size is represented by a unique distribution function. This distribution function for large particles can be obtained from the maximum height and entrainment rate equations, i.e., Eq. 1 and 2. Here an assumption is made that the decrease in the solid entrainment rate for large particles is due to the distribution of initial solid velocity (George and Grace, 1980). Figure 1 and 2 illustrate the calculation procedure for entrainment of limestone particles from a fluidized bed combustor. There are three steps in this calculation to obtain initial solid velocity distribution:

(a) Calculate the relation between h_{max} and U_{io} Eq. 2 for particle size dp_i. (Figure 1-a)

(b) Set up flux profile of Fi/F_{io} vs. h from Eq. 1 as in Figure 1-b. The curve of the cumulative weight fraction, F_i/F_{io}, vs. freeboard height, h, is independent of particle size for large particles due to the fact that the large particles have the following flux equation as shown in Figure 1-b.

$$F_i/F_{io} = \exp(-6.4\, h) \quad (6)$$

(c) Combine (a) and (b) by plotting the relation of U_{io} vs. F_i/F_{io}. This gives the cumulative distribution of the ejected particle velocities. For example, as shown in Figure 1-b, the h_{max} for the 200 μm limestone particles with initial velocity equal to 2 m/s is 0.23 m. At this height the particle entrainment rate is 21% of the entrainment rate at the bed surface. (Figure 1-b, F_i/F_{io})

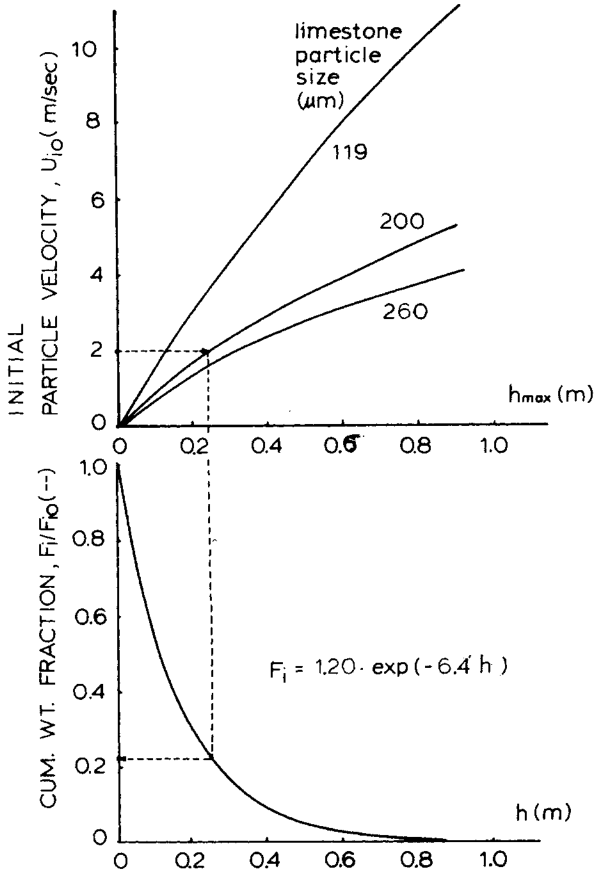

Figure 1. Procedure for calculating the initial velocity for the particles with terminal velocity larger than the gas velocity. (a) Initial solid velocity for the particle to reach different heights; (b) weight fraction of particles at different heights.

The examples shown in Figures 1 and 2 are for limestone particles ranging from 119 to 250 μm in size with the superficial gas velocity of 0.3 m/s. In comparison with the bubble velocity at the bed surface, the initial solid velocity distribution is seen to range from 0 to 8 times the bubble velocity depending on the size of the ejected particles. For the small particles, the average value of the initial velocity is higher than that of large particles.

For those fine particles with terminal velocity less than the gas velocity, the initial solid velocity distribution is taken to have an average value of 2.1 times the bubble velocity at the bed surface, as proposed by George and Grace (1978).

Solid Hold-Up. In order to simulate the solid-gas reaction in the freeboard, it is necessary to estimate the solid hold-up or solid concentration in the freeboard. The hold-up of the particles in the freeboard is calculated by knowing the relation between the solid flux and the solid velocity, both upward and downward. The particles' hold-up is defined as follows:

$$dH_{di} = \frac{dF_i}{U_{si}} + \frac{dF_i'}{U_{si}'} \quad (7)$$

Accordingly, if the solid velocity is a constant at different heights, the solid sold-up can be represented by the following equation:

$$H_{di} = F_i/U_{si} + F_i'/U_{si}' \quad (8)$$

However, if the solid velocity is a distribution, the calculation should be done in the following way:

$$H_{di} = H_{di,asc} + H_{di,des}' = \int_0^{F_i} \frac{dF_i}{U_{si}} + \int_0^{F_i'} \frac{dF_i'}{U_{si}'} \quad (9)$$

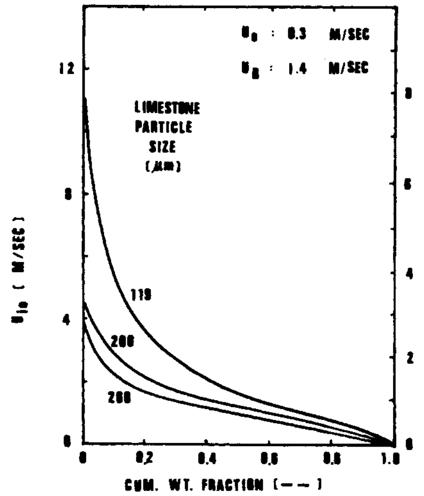

Figure 2. Initial solid velocity distribution for limestone particles (U_o = 0.3 m/s, U_B = 1.4 m/s).

Here, U_{si} and U'_{si} are the solid ascending and descending velocities and F_i and F'_i are the ascending and descending flow rates of particles, respectively. The downward flow rate of particles, F'_i, is obtained from the material balance of the particles in the freeboard as:

$$F'_i = (F_{io} - F_{i\infty})\exp(-ah) \tag{10}$$

Figure 3 illustrates the calculation steps for the estimation of solid hold-up of 119 μm limestone in the freeboard. The initial solid velocity distribution for this case is shown in Figure 2.

(a) Calculate the velocity distribution profiles, both upward and downward, from Eq. 2 at the height, h, above the bed surface.

(b) Estimate the solid hold-up from Eq. 9 by integrating the area under the curve $1/U_{si}$ vs. F_i and $1/U'_{si}$ vs. F'_i to this height.

(c) Establish the solid hold-up profile along the freeboard by repeating steps (a) and (b) for different heights.

The total solid hold-up in the freeboard (H_d) is the summation of the hold-up for each particle size (H_{di}) as:

$$H_d = \sum_i H_{di} \tag{11}$$

Reaction Model—Axial Dispersion

In a steady-state flow, the material balance equation for any reactant species i in a reactor with the length H can be derived based on the convection and the axial dispersion flow as follows (Danckwerts, 1953):

$$E_Z \frac{d^2C_i}{dh^2} - U_g \frac{dC_i}{dh} + R_i = 0 \tag{12}$$

where R_i is the production rate of species i and E_Z is the axial dispersion coefficient which can be estimated from the Peclet number of the gas flow in the freeboard region (Wen and Fan, 1975; Rajan and Wen, 1980).

Langmuir's "closed-closed vessel" boundary conditions are used for this case (Langmuir, 1908). If the reaction rate is constant, the analytical solution of the concentration profile for the first-order reaction is given by Danckwerts (1953).

For a homogeneous reaction, the overall reaction rate, R_i, is a function of temperature and gas concentration; for a heterogeneous reaction, however, R_i is also a function of the number of particles, particle size, etc. The forms of R_i used for the freeboard reactions are discussed later.

The axial dispersion model has a similar flow characteristic as the compartment-in-series with back flow model. In actuality, the axial dispersion model is roughly equivalent to the compartment-in-series model with $(1 + U_gH/2E_Z)$ equal to the number of equal-sized compartments (Wen and Fan, 1975). Both models

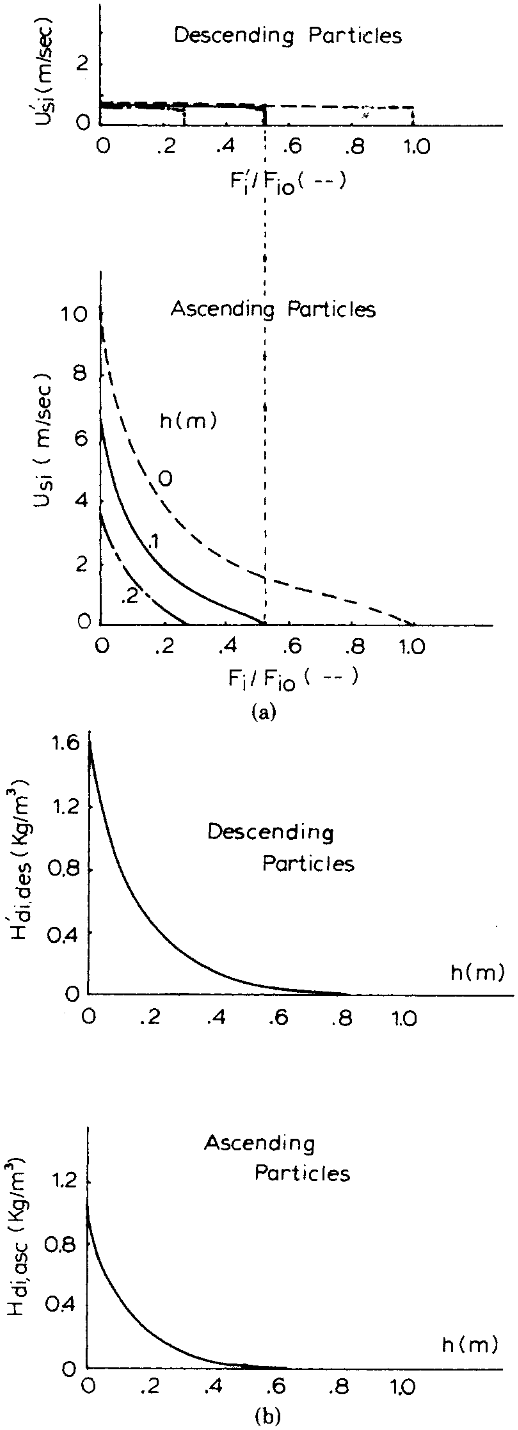

Figure 3. Procedure for calculating the solid hold-up of large particles (limestone particle size = 119 μm, U_o = 0.3 m/s): (a) the solid velocity distribution at different heights; (b) the solid hold-up for the ascending and descending particles.

lead to the two limiting cases of ideal flow model, i.e., the plug flow model when $E_Z \to 0$ and the complete-mixing flow model when $E_Z \to \infty$.

DISCUSSION

Freeboard Catalytic Gas-Phase Reaction

For a catalytic gas-phase reaction, the overall reaction rate constant, k_{ov}, consists of three resistances: one due to the gas film, another due to the pores inside the particle and the third due to the

TABLE 1. DATA FOR FLUIDIZED BED CATALYTIC GAS PHASE REACTION

Bed temperature (T)	400°C
Bed diameter (D_c)	1 m
Settled bed height	1 m
Mean projected particle diameter (dp)	100 μm
Particle bulk density (ρ_s)	2000 kg/m^3
Minimum fluidization velocity (U_{mf})	0.01 m/sec
Mean bubble diameter at the bed surface (D_B)	0.30 m
Emulsion phase voidage (ϵ_{mf})	0.5
Packed bed voidage (ϵ_m)	0.45
Fluidizing gas viscosity at 400°C (μ)	2.67×10^{-5} kg/m sec
Fluidizing gas density at 400°C (ρ_g)	0.487 kg/m^3
Reactant gas diffusivity (D)	2.07×10^{-5} m^2/sec
Fluidizing gas velocity (U_o)	2 m/sec
Freeboard height (H)	1 m
Reaction rate constant, (k_t)	5 sec^{-1}
Reaction (1st order)	A → B

$$\text{Overall reaction rate expression} = \frac{(1-\epsilon)}{\dfrac{dp}{6h_m} + \dfrac{(1-\epsilon_m)}{k_t}}$$

chemical reaction. For a volumetric reaction, the resistance due to the gas film is negligible compared to the gas diffusion resistance through the pores. However, for a surface reaction on a nonporous catalyst, the diffusion through the pores is neglected.

The resistance due to the mass transfer of the reactant through the gas film can be represented by the term: $\Sigma_i Y_i(dp_i/6h_{mi})$, where Y_i is the weight fraction of the particle size dp_i in the freeboard h meters above the bed surface. h_{mi} is the mass transfer coefficient across the gas film and can be estimated from the equation given by Rowe et al. (1965):

$$\frac{h_m dp}{D} = 2 + 0.69\left(\frac{\mu}{\rho_g D}\right)^{1/3}\left(\frac{(U_o - U_{ts})\,dp\,\rho_g}{\mu}^{1/2}\right) \tag{13}$$

The aforementioned chemical reaction rate represents the intrinsic rate, k_t, which can be expressed in an Arrhenius' form:

$$k_t = k_{to}\exp(-E/RT) \tag{14}$$

For the volumetric reaction, k_t is independent of the particle size; for the surface reaction, however, k_t is a function of total surface area, S.

Thus, for a first order reaction, R_i can be represented by the following equation:

$$R_i = -k_{ov}\cdot C_i(1-\epsilon) \tag{15}$$

and, for the surface reaction

$$k_{ov} = \frac{1}{\sum_i Y_i \cdot \dfrac{dp_i}{6h_{mi}} + \dfrac{(1-\epsilon)}{k_s \cdot S}} \tag{16}$$

for volumetric reaction

$$k_{ov} = \frac{1}{\sum_i Y_i\left(\dfrac{dp}{6D_{\text{eff}}}\right)_i + \dfrac{1}{k_t}} \tag{17}$$

Here, D_{eff} is the gas diffusivity through the pores. ϵ, the voidage in the freeboard, can be calculated from the solid hold-up or solid concentration (H_d) as follows:

$$\epsilon = 1 - \frac{H_d}{\rho_s} \tag{18}$$

Finally, the concentration profile of the reactant can be obtained by solving the material balance equation, i.e., Eq. 12, or using the approximation of the analytical solution for constant reaction rate solved by Danckwerts (1953). Since the reaction rate constant in the freeboard is not a constant, the approximation should be used with caution. In this study, the approximated method was used to calculate the concentration profile of the reactant in the freeboard.

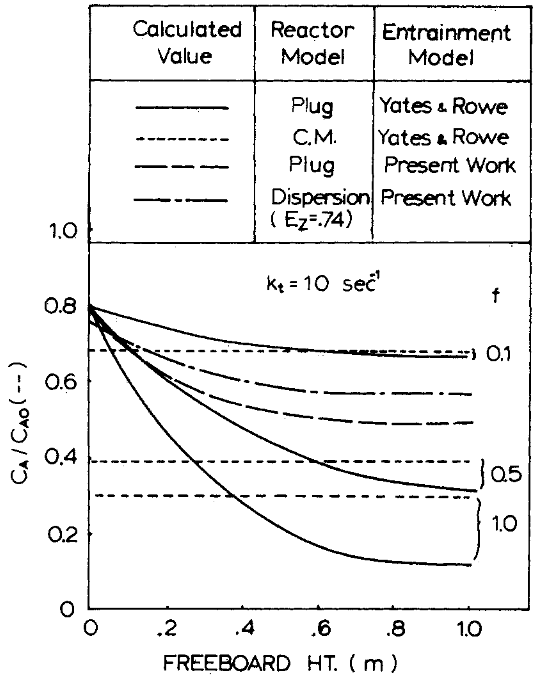

Figure 4. Comparison of the concentration profiles in the freeboard calculated from the model by Yates and Rowe (1977) with those calculated from the present model for the catalytic gas phase reaction.

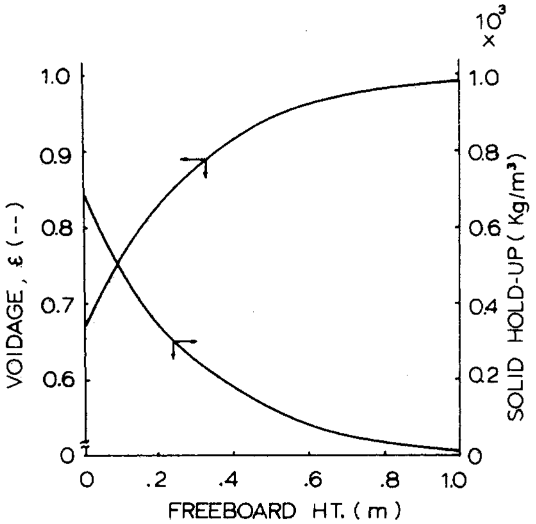

Figure 5. Profiles of solid hold-up and voidage in the freeboard.

The gas concentration at height $(h + \Delta h)$ is calculated as follows:

$$C_A\,(h + \Delta h) = C_A(h) + \Delta C_A \tag{19}$$

$$\Delta C_A = C_A(h)|_{\text{with } k_{ov} = k_{ov}(h)} - C_A(h)|_{\text{with } k_{ov} = k_{ov}(h+\Delta h)} \tag{20}$$

This approximation is valid only when the step size (Δh) is taken very small or $C_A(h) = C_A(h + \Delta h)$. In this study, the step size used in the approximation is 0.01 cm. This gives less than 5% difference in the outlet gas concentration compared to the calculated value obtained by solving Eq. 12 numerically.

Comparison of Present Calculation with Literature. In order to demonstrate the characteristic of the freeboard model proposed, a simple example given by Yates and Rowe (1977) was recalculated based on the present model. The data used in the calculation is listed in Table 1. Figure 4 shows the freeboard concentration profile calculated from this model and compared to that calculated from the complete-mixing and plug flow model proposed by Yates and Rowe (1977). In the model proposed by Yates and Rowe (1977), the solid entrainment rate is assumed constant and equal to a fraction (f) of the total amount of particles in the wake of the erupted bubbles. The projected particle velocity was also assumed to be a constant value, i.e., $(U_o - U_{ts})$. However, in the present model, the solid entrainment rate decreases exponentially along the freeboard. The solid particles are ejected to the freeboard with different initial velocities and the descending particles along the wall fall down at the terminal velocity. The voidage in the freeboard thus increases as the particle concentration decreases along the freeboard as shown in Figure 5. Since the overall reaction rate constant is proportional to the solid hold-up in the freeboard or $(1 - \epsilon)$, the concentration profile calculated in this way resembles the characteristics of the solid hold-up curve. In order to compare the present entrainment model with that proposed by Yates and Rowe (1977), the plug flow concentration profile based on the present solid entrainment model is also shown in Figure 4. The comparison shows that the present entrainment model eliminates the parameter, f, necessary in the model proposed by Yates and Rowe (1977). This parameter is sensitive to the gas concentration profile, especially at the high reaction rate constant.

Fluidized Bed Coal Combustion Freeboard Reactions

In the fluidized bed coal combustor, the freeboard region provides additional opportunities for solid-gas reactions such as char combustion, SO_2 absorption and NO_x reduction. In order to evaluate the extent of the freeboard reactions, it is necessary to estimate the solid hold-up of sorbent particles (CaO) as well as char (C) particles in the freeboard. These particles in the freeboard are thrown up from the bed due to the bursting of bubbles at the bed surface. The amount of projected particles is related to the particle size distribution in the bed. In this study, the method developed by Rajan and Wen (1980) was used to calculate the particle size distribution in the bed. This calculation is based on the mass balance of each of the close-out particle size fractions in the bed. The mass balance is made for the particles fed or recycled to the bed, the particles elutriated or withdrawn from the bed and the attrition in the bed.

The reaction kinetics of char combustion, SO_2 absorption and NO_x reduction used by Rajan and Wen (1980) for fluidized bed combustor modeling are used in this study. However, the material balance equations for both the gas phase (SO_2 and NO_x) and the solid phase (CaO and C) based on the up-going, down-coming and recycled particles are listed in Table 2. The solid entrainment and hold-ups for limestone and char particles are calculated first using Eqs. 1 to 11 and Eq. viii in Table 2. The gas concentrations of SO_2 and NO_x are then obtained for Eqs. i and iv in Table 2. The particle temperatures used in all calculations are taken directly from the experimental data. However, in the case of over-bed recycle, the temperature profile of the recycled limestone particles is calculated from Eq. ix in Table 2. Finally, solid conversions of limestone particles moving up, down and recycled are calculated from Eqs. v and vii in Table 2. In this calculation, calcium conversion of the recycled stream is assumed (if no recycle, $x^r_{io,\ell} = 0$). Iteration of these calculation procedures at different heights is performed until the outlet of the freeboard is reached. For the case with recycling of fine particles, the calcium conversion of the recycled particles (x^R_i) can be calculated from Eq. xi in Table 2 and compared with the calcium conversion assumed for the recycled particles ($x^r_{io,\ell}$). The whole calculation is repeated, if the assumed value of the calcium conversion of recycled particles ($x^r_{io,\ell}$) does not match the calculated value (x^R_i).

Comparison of Present Calculation with Experimental Data. The freeboard reactions of B & W's 6 ft × 6 ft (1.8 m × 1.8 m) fluidized bed combustor (B & W, 1979) were simulated and the results were used to test the validity of the proposed model. In the operation of this FBC, the bed height is kept about 4 ft (1.2 m), which is just high enough to immerse all the heat transfer tubes in the bed. The freeboard height of this unit is 36 ft (11 m) with two bundles of heat transfer tubes each occupying the space 3.5 ft (1.1 m) in height situated at about 18 ft (5.5 m) above the bed surface.

TABLE 2. EQUATIONS FOR THE FBC FREEBOARD MODEL

1) Material Balance Equations

Gas phase:

$$SO_2: E_z \frac{d^2C_{SO_2}}{dh^2} - U_o \frac{dC_{SO_2}}{dh} + R_{SO_2} = 0 \qquad \text{(i)}$$

$$NO_x: E_Z \frac{d^2C_{NO_x}}{dh^2} - U_o \frac{dC_{NO_x}}{dh} + R_{NO_x} = 0 \qquad \text{(ii)}$$

where

$$R_{SO_2} = \sum_i R_{SO_{2,i}}$$

$$\text{and } -R_{SO_{2,i}} = k^u_{vl,i} \cdot C_{SO_2} \cdot (1 - \epsilon^u_{i,l}) + k^d_{vl,i} \cdot C_{SO_2} \cdot (1 - \epsilon^d_{i,l}) + k^r_{vl,i} \cdot C_{SO_2} \cdot (1 - \epsilon^r_{i,l}) \qquad \text{(iii)}$$

$$R_{NO_x} = \sum_i R_{NO_{x,i}}$$

$$\text{and } -R_{NO_{x,i}} = \frac{6}{dp_i} C_{NO_x} \cdot k_{NO_x} [(1 - \epsilon^u_{i,c}) + (1 - \epsilon^d_{i,c}) + (1 - \epsilon^r_{i,c})] \qquad \text{(iv)}$$

Solid phase:

$$\text{Limestone: } \frac{d(F^u_{i,l} \cdot x^u_{i,l})}{dh} \frac{M_s}{M_{CaSo_4}} = k^u_{vl,i} \cdot C_{SO_2} \cdot (1 - \epsilon^u_{i,l}) \cdot M_s \qquad \text{(v)}$$

$$-\frac{d(F^d_{i,l} \cdot x^d_{i,l})}{dh} \frac{M_S}{M_{CaSO_4}} = k^d_{vl,i} \cdot C_{SO_2} \cdot (1 - \epsilon^d_{i,l}) \cdot M_S \qquad \text{(vi)}$$

$$\frac{d(F^r_{i,l} \cdot x^r_{i,l})}{dh} \frac{M_S}{M_{CaSO_4}} = k^r_{vl,i} \cdot C_{SO_2} \cdot (1 - \epsilon^r_{i,l}) \cdot M_S \qquad \text{(vii)}$$

Carbon:

$$\frac{dF^u_{i,c}}{dh} - \frac{dF^d_{i,c}}{dh} + \frac{dF^r_{i,c}}{dh} = R_{c,i} \qquad \text{(viii)}$$

2) Temperature profile for the overbed recycled particles (consider only the convective and radiative heat transfers between recycled fine particles and the gas phase)

$$\frac{d\,T_{s,i}}{dh} = \frac{6(1 - \epsilon^r_i)}{dp_i C_{p_s} F^r_{i,l}} [h_c(T_g - T_{s,i}) + a(\epsilon_g T^4_g - \alpha_g \epsilon_s T^4_{s,i})] + \frac{\Delta H^r_{rxn,l}}{C_{p_s} \cdot F^r_{i,l}} \frac{d(F^r_{i,l} \cdot x^r_{i,l})}{dh} \qquad \text{(ix)}$$

$$\text{where } \frac{h_c \cdot dp_i}{k_g} = N_u$$

$$C_{ps} = 0.2 + 0.00088\,[T_{s,i}(^\circ k) - 273] \left(\frac{kcal}{Kg\,^\circ K}\right) \qquad \text{(x)}$$

3) Calcium Conversion of Recycled Limestone Particles

$$x^R_i = \frac{x^u_{i,l}(H) \cdot F^u_{i,l}(H) + x^r_{i,l}(H) F^r_{i,l}(H)}{F^u_{i,l}(H) + F^r_{i,l}(H)} \qquad \text{(xi)}$$

LIMESTONE AND COAL FEED SIZE DISTRIBUTION:

size (μm)	limestone feed size cum. wt. %	coal feed size cum. wt. %
9500	100.0	100.0
6350	100.0	100.0
4750	99.8	98.9
2380	84.3	83.6
1190	62.5	61.5
595	40.6	38.9
297	24.9	21.5
149	15.8	10.5
74	11.3	5.6
44	11.3	2.8

Table 3 shows typical operating conditions for the B & W FBC. Figure 6 shows the comparison of the calculated particle-size distribution with the experimental data under this set of operating

Table 3. Typical Operating Condition of Babcock & Wilcox Fluidized Bed Combustor.

Bed temperature	1558.4°F	(1121°K)
Bed dimension	6′ × 6′	(1.8 × 1.8 m)
Expanded bed height	49.7″	(1.3 m)
Fluidized gas velocity (air)	7.5 ft/sec	(2.3 m/sec)
Coal feed rate (Ohio #6)	1968 lb/hr	(0.248 kg/sec)
Limestone feed rate (Lowellville)	771 lb/hr	(0.097 kg/sec)
FBC total height	40′	(12 m)
No recycle		
Distributor	0.0938″ (0.238 cm) holes on 0.587″ (1.49 cm) square pitch	

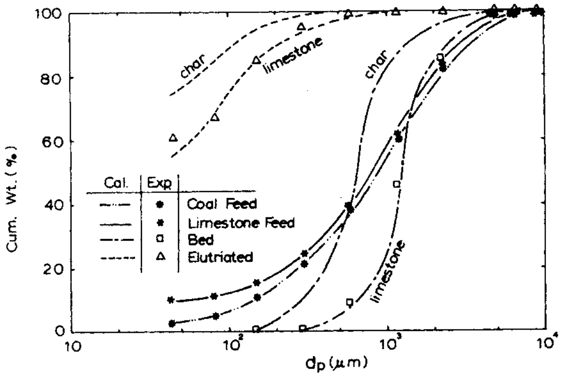

Figure 6. Size distribution of the particles in the B & W FBC (operating conditions listed in Table 6).

Table 4. Comparison of Calculated and Experimental Elutriation from the Babcock and Wilcox Fluidized Bed Combustor.
(Operating Conditions are Listed in Table 3)

	Amount of particles elutriated (10^3 kg/sec) Calculated	Experimental
Limestone	47.12	46.12**
Char	14.87	15.37*
Total	61.99	61.49

* Estimated from the analysis data of 25% carbon content in the particles elutriated.
** Estimated by subtracting the amount of char from the total amount elutriated.

conditions. As can be seen from this figure, most of the fine particles (particle size ranging from 0 to 595 μm) elutriated from the bed, either supplied from the feed stream or generated from the abrasion of large particles in the bed. Table 4 shows the comparison of the amount of elutriated particles calculated from the proposed model, Eqs. i–viii in Table 2, with the experimental data. The agreement appears good. In this calculation, the solid hold-ups of both limestone and char particles in the freeboard are also estimated. The hold-up of char particles is dependent on the residence time of char particles in the freeboard and burning time of the char particles. Char particles are either partially or completely burnt in the bed and the unburnt char particles are elutriated (Rajan and Wen, 1980). Based on the solid hold-up information, the concentration profiles of SO_2 and NO_x can be obtained from the material balance equations of both gas and solid phases. These material balance equations are shown in Table 2. In all the calculations, the concentrations of SO_2 and NO_x at the bed surface are estimated from the FBC model developed by Rajan and Wen (1980). The conversion of CaO to $CaSO_4$ in the bed (x_t), on the other hand, is calculated from the experimental data for all the cases including overbed, underbed and without recycle. The calculated concentration profiles of SO_2 and NO_x in the freeboard are compared with experimental data in Figures 7 and 8 for both cases with and without recycling of fine particles. The rapid decrease of the SO_2 and NO_x concentration from the bed surface as the gas moves up above the bed is due to the large amount of entrained particles in the freeboard, especially near the bed surface. When the fine particles are recycled, the amount of sorbent particles as well as

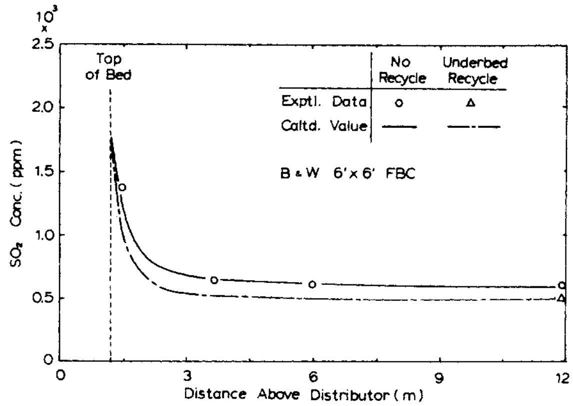

Figure 7. SO_2 absorption profile in the B & W FBC.

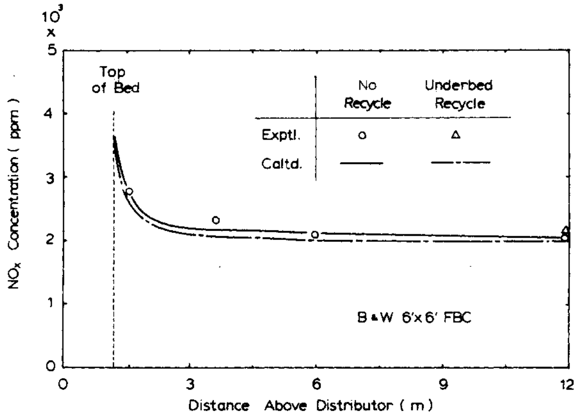

Figure 8. NO_x reduction profile in the B & W FBC.

Table 5. Comparison of the Outlet Concentrations of SO_2 and NO_X from the Babcock and Wilcox Fluidized Bed Combustor.

Test No.		Outlet concentration (ppm) SO_2	NO_x
8-6*,	Experimental	593–627	215–247
No recycle	Average	610	232
	Calculated	603	226
8-3*,	Experimental	478–521	216–232
underbed recycle,	Average	496	227
recycle rate = 0.153 kg/sec	Calculated	501	214
10-1**	Experimental	1124–2054	276–322
overbed recycle	Average	1405	293
recycle rate = 0.277 kg/sec	Calculated	1369	301
10-2**	Experimental	560–1283	259–292
underbed recycle,	Average	867	279
recycle rate = 0.165 kg/sec	Calculated	913	280

* Sulfur content in the feed coal: 3.7% in wt.
** Sulfur content in the feed coal: 4.5% in wt.

char particles in the freeboard is increased. Therefore, more char particles are burnt in the freeboard and the SO_2 absorption and NO_x reduction are also improved. It is noted that the temperature in the region of the freeboard near the bed surface is higher than the temperature inside the bed due to the additional combustion of char particles in the freeboard. The rise in temperature in the freeboard is greater when fine particles are recycled.

The combustion of the calculated outlet concentrations of SO_2 and NO_x with and without recycle and those of experimental data is shown in Table 5. It is noted that the reinjection point of the fine particles does affect the outlet SO_2 concentration. The outlet SO_2 concentration is lower for the underbed recycle than for the overbed recycle due to the additional heat-up period of the reinjected limestone particles inside the bed. The recycled limestone temperature is estimated from Eq. ix shown in Table 2. Since the overall heat transfer coefficient for the particles inside the bed is much higher than that in the freeboard, the calculated recycled particle temperature at the bed surface is very close to the gas temperature emerging from the bed. Thus, the underbed recycled particle temperature in the freeboard can be approximated by the gas temperature without creating any significant errors in the calculation of the SO_2 concentration profile in the freeboard.

In all cases examined, it is noted that a large amount of SO_2 is removed in the freeboard. In some cases the data showed that up to 40% of the total SO_2 removal is achieved in the freeboard. Such an unusually large amount of SO_2 absorption in the freeboard is due to the high gas velocity and the large amount of entrainment of limestone fines produced as the result of attrition. Most of the SO_2 appears to be absorbed very near the surface of the bed where large amounts of particles are splashed and subsequently returned to the bed. However, because of the difficulty in identifying the exact bed height, accurate assessment of the freeboard contribution is not possible.

ACKNOWLEDGMENT

This work was partially supported by a grant from the Energy Research Center of West Virginia University and a grant from the Department of Energy, United States Government.

NOTATION

a	= constant in the entrainment equation (L/m)
C_D	= drag coefficient for multiparticle system
C_{DS}	= drag coefficient for single particle
C_i	= concentration of species i (kg mol/m^3)
C_{io}	= concentration of species i at the bed surface (kg mol/m^3)
C_{ps}	= heat capacity of solid particles (J/kg·K)
D	= gas diffusivity (m^2/s)
d_p or d_{pi}	= particle diameter of close-cut particle i (m)
D_B	= bubble diameter at the bed surface (m)
D_c	= column diameter (m)
D_{eff}	= effective diffusivity through the pores (m^2/s)
E	= activation energy (J/kg mol)
E_Z	= axial dispersion coefficient (m^2/s)
f	= fraction of wake solids ejected into freeboard
F_i	= entrainment rate of particle size i (upward) (kg/m^2·s)
F_i'	= entrainment rate of particle size i (downward) (kg/m^2·s)
F_{io}	= entrainment rate of particle size i at the bed surface (kg/m^2·s)
$F_{i\infty}$	= elutriation rate of particle size i (kg/m^2·s)
g	= gravitational acceleration constant (m/s^2)
H	= total freeboard height (m)
ΔH_{rxn}	= heat of reaction (J/kg)
h	= height above the dense bed surface (m)
h_c	= convective heat transfer coefficient (J/m^2·h·K)
H_d	= total solid hold-up (kg/m^3)
H_{di}	= solid hold-up for particle size i (due to upward particles) (kg/m^3)
H_{di}'	= solid hold-up for particle size i (due to downward particles) (kg/m^3)
h_m	= mass transfer coefficient through the gas film (m/s)
$h_{\max}$	= maximum projected height of solid particles (m)
k_g	= thermal conductivity of gas phase (J/h·m·K)
k_{ov}, k_v	= overall reaction rate constant (L/s)
k_s	= surface reaction rate constant (L/m^2·s)
k_t	= intrinsic reaction rate constant (L/s)
k_{to}	= pre-exponential reaction rate constant (L/s)
M_i	= molecular weight of species i (kg/kg mol)
N_{Re}	= particle Reynolds number = $\dfrac{\rho_g \cdot dp \lvert U_{sr} \rvert}{\mu}$
N_u	= Nusselt number = $\dfrac{h_c \cdot dp_i}{k_g}$
R	= gas constant = 8319.17 (J/kg mol·K)
R_i	= production rate of species i $\left(\dfrac{\text{kg mol}}{\text{m}^3\cdot\text{s}}\right)$
S	= total particle surface area (m^2)
t	= time (s)
T	= reaction temperature (K)
T_g	= gas temperature (K)
T_s	= solid temperature (K)
U_B	= bubble velocity at the bed surface (m/s)
U_g	= interstitial gas velocity = U_o/ϵ (m/s)
U_{io}	= initial solid velocity (at the bed surface) (m/s)
U_{mf}	= minimum fluidization gas velocity (m/s)
U_o	= superficial gas velocity (m/s)
U_{si}	= solid velocity (upward) (m/s)
U_{si}'	= solid velocity (downward) (m/s)
U_{sr}	= particle velocity relative to the gas stream (m/s)
U_{ts}	= single particle terminal velocity of particle size i (m/s)
x_i	= calcium conversion of CaO to $CaSO_4$
X_i	= weight fraction of particle size i in the bed
X_{io}	= initial weight fraction of particle size i in the bed
Y_i	= weight fraction of particle-size dpi in the freeboard

Greek Letters

α_g	= absorptivity of the gas
ϵ	= voidage in the freeboard
ϵ_g	= emissivity of the gas
ϵ_i	= voidage in the freeboard for the system having only particle size i
ϵ_m	= pack back voidage
ϵ_{mf}	= emulsion phase voidage in the bed
ϵ_s	= emissivity of the solid
σ	= radiation heat transfer constant (J/h·K^4·m^2)
ρ_g	= gas density (kg/m^3)
ρ_s	= solid density (kg/m^3)
μ	= viscosity of gas (kg/m·s)

Subscripts

c	= char particle
ℓ	= limestone particle

Superscripts

d	= falling down particles
r	= recycled particles (in the freeboard)
R	= recycled particles (in the outlet)
u	= going up particles

LITERATURE CITED

Babcock & Wilcox, B & W, "Fluidized Bed Combustion Development Facility and Commercial Utility AFBC Design Assessment," Quarterly Technical Progress Report prepared for EPRI, Contract No. RP-718-2 (Jan.–Mar., 1979).

Beer, J. M., A. F. Sarofim, P. K. Sharma, T. Z. Chaung, and S. S. Sandhu, "Fluidized Coal Combustion: The Effect of Sorbent and Coal Feed Particle Size upon the Combustion Efficiency and NO_x Emission," *Fluidization*, eds., J. R. Grace and J. M. Matsen, Plenum Press, New York and London, 185 (1980).

Danckwerts, P. V., "Continuous Flow Systems—Distribution of Residence Times," *Chem. Eng. Sci.*, **2**, 1 (1953).

Do, H. T., J. R. Grace, and R. Clift, "Particle Ejection and Entrainment from Fluidized Beds," *Powder Technol.*, **6**, 195 (1972).

Ford, W. D., R. C. Reineman, I. A. Vasalos, and R. J. Fahrig, "Operating Cat Crackers for Maximum Profit," *Chem. Eng. Prog.*, **73**, No. 4, 92 (1977).

Fournol, A. B., M. A. Bergougnou, and G. G. J. Baker, "Solid Entrainment

in a Large Gas Fluidized Bed," *Can. J. of Chem. Eng.*, **51**, 401 (1973).
George, S. E., and J. R. Grace, "Entrainment of Particles from Aggregative Fluidized Beds," *AIChE Symp. Ser.*, **74**, No. 176, 67 (1978).
Horio, M., A. Taki, Y. S. Hsieh, and I. Muchi, "Elutriation and Particle Transport Through the Freeboard of a Gas-Solid Fluidized Bed," *Fluidization*, eds., J. R. Grace and J. M. Matsen, Plenum Press, New York and London, 509 (1980).
Langmuir, I. J., "The Velocity of Reaction in Gases Moving Through Heated Vessels and the Effects of Convection and Diffusion," Amer. Chem. Soc., **30**, 1742 (1908).
de Lasa, H. I., and J. R. Grace, "The Influence of the Freeboard Region in a Fluidized Bed Catalytic Cracking Regenerator," *AIChE J.*, **25**, No. 6, 984 (1979).
Matsen, J. M., "Entrainment Research: Achievements and Opportunities," Proceedings of NSF Workshop on Fluidization, H. Litman, p. 452 (1979).
Miyauchi, T., and S. Furusaki, "Relative Contribution of Variables Affecting the Reaction in Fluid Bed Contractors," *AIChE J.*, **20**, No. 6, 1087 (1974).
Rajan, R. R., and C. Y. Wen, "A Comprehensive Model for Fluidized Bed Coal Combustors," *AIChE J.*, **26**, No. 4, 642 (1980).
Rowe, P. N., K. T. Claxton, and J. B. Lewis, "Heat and Mass Transfer from a Single Sphere in an Extensive Flowing Fluid," *Trans. I. Chem. E.*, **43**, T14 (1965).
Wen, C. Y., *Dilute and Dense Phase Pneumatic Transport*, Chapter in "Bulk Materials Handling," **1**, ed., M. C. Hawk, University of Pittsburgh, 258 (1971).
Wen, C. Y., and L. H. Chen, "A Fluidized Bed Combustor Freeboard Model," The Proceedings of the 6th International Conference on Fluidized Bed Combustion, **III**, 1115 (1980).
Wen, C. Y., and L. H. Chen, "Fluidized Bed Freeboard Phenomena—Entrainment and Elutriation," *AIChE J.* (Jan., 1982).
Wen, C. Y., and L. T. Fan, "Model for Flow Systems and Chemical Reactors," Marcel Dekker, Inc., New York (1975).
Wen, C. Y., and R. F. Hashinger, "Elutriation of Solid Particles from a Dense Phase Fluidized Bed," *AIChE J.*, **6**, No. 2, 220 (1960).
Wen, C. Y., and W. S. O'Brien, *Pneumatic Conveying and Transporting*, Chapter 3 in "Gas-Solids Handling in the Process Industries," eds., J. M. Marchello and A. Gomezplata, Marcel Dekker, Inc., 89 (1976).
Yates, J. G., and P. N. Rowe, "A Model for Chemical Reaction in the Freeboard Region Above a Fluidized Bed," *Trans. Instn. Chem. Engrs.*, **55**, 137 (1977).
Zenz, F. A., and N. A. Weil, "A Theoretical-Empirical Approach to the Mechanism of Particle Entrainment from Fluidized Beds," *AIChE J.*, **4**, No. 4, 472 (1958).

Manuscript received June 16, 1981; revision received February 4, and accepted February 22, 1982

R & D NOTES

Polarographic Technique for the Determination of Effective Surface Area of Electrodes

R. J. LUTZ, ARUN MENAWAT, and J. I. PETERSON

Biomedical Engineering and Instrumentation Branch
Division of Research Services
National Institutes of Health
Bethesda, MD 20205

INTRODUCTION

This paper describes a voltage-sweep polarographic method for determining the effective surface area of metal electrodes *in situ*. Sawyer and Roberts (1974) discuss the notion that the real or true surface area of a solid electrode can differ from its projected or geometric area because of surface roughness. This is particularly true for platinized platinum electrodes. Situations may arise where the surface of an electrode has an irregular geometry which makes micrometer or optical measurements difficult. In our own recent work, platinum electrodes involved in an experiment are not easily accessible for visual area measurements. The polarographic technique that we have utilized is a simple and reliable method which overcomes these difficulties. It has potential application in microelectrode studies where surface area is a required parameter.

BACKGROUND

The area measurement method is particularly relevant to work in our laboratory that has involved the measurement of wall shear stress and mass transfer coefficients in plastic models of arterial geometries with the goal of understanding the interrelationship of fluid flow and the initiation of atherosclerosis (Lutz et al., 1977). Wall shear stress and mass transfer coefficients were measured using an electrochemical technique described by Hanratty and co-worker for turbulence measurements in pipes (Fortuna and